available at www.sciencedirect.com

ScienceDirect

www.elsevier.com/locate/brainres

BRAIN RESEARCH

Research Report

Increased nitric oxide levels and nitric oxide synthase isoform expression in the cerebellum of the taiep rat during its severe demyelination stage

Bertha Alicia Leon-Chavez[a], *Patricia Aguilar-Alonso*[a], *Juan Antonio Gonzalez-Barrios*[b,e], *J.Ramón Eguibar*[c], *Araceli Ugarte*[c], *Eduardo Brambila*[a], *Alejandro Ruiz-Arguelles*[d], *Daniel Martinez-Fong*[e,*]

[a]*Facultad de Ciencias Químicas, BUAP, 14 sur y Av. San Claudio, Edif. 138, San Claudio, 72570 Puebla, Pue., México*
[b]*División de Medicina Genómica del Hospital regional 1° de Octubre, ISSSTE, Avenida Instituto Politécnico Nacional 1669, México D.F. 07760, México*
[c]*Instituto de Fisiología, BUAP, 14 sur, 6103, Puebla, Pue., México*
[d]*Laboratorios Clínicos de Puebla, Blvd. Díaz Ordaz No. 808. Col. Anzures, Puebla, PUE. C.P. 72530, México*
[e]*Departamento de Fisiología, Biofísica y Neurociencias, Cinvestav, Apdo. Postal 14-740, México D.F. 07000, México*

ARTICLE INFO

Article history:
Accepted 25 August 2006
Available online 3 October 2006

Keywords:
Hypomyelination
Nitrite
Glial activation
Reactive astrocytosis
Microglia cell
Neuroimmunology

ABSTRACT

We have previously reported progressive reactive astrocytes in the cerebellum of taiep rats, one of the most regions affected by demyelination, and activation of cerebellar glial cells in vitro. Based on the hypothesis that activated glial cells produce high levels of reactive nitrogen intermediates, we assessed the production of nitric oxide (NO) and the expression of the three NO synthases (NOS) in the cerebellum of 6-month-old taiep rats. A significant 40% increase of NO levels was measured in taiep rats when compared with controls. The protein and mRNA levels of the three NOS isoforms were also significantly increased. In contrast to controls, immunostaining assays against nNOS or iNOS showed an increased number of immunoreactive glial cells in the granular layer (nNOS) and Purkinje layer (iNOS) of cerebellum of taiep rats. Microglia–macrophages and both CD4- and CD8-immunoreactive cells were observed in cerebellar white matter of taiep rats only, thus suggesting other possible cell sources of those NOSs. Differences in the cellular location for eNOS immunoreactivity were not observed. The enhanced levels of NO, NOS proteins, mRNAs, and NOS immunoreactivities in glial cells and microglia strongly suggest glial activation together with the professional immune cells can aggravate the demyelination of aged taiep rats.

* *Corresponding author*. Fax: +52 55 5061 3754.
E-mail address: dmartine@fisio.cinvestav.mx (D. Martinez-Fong).

0006-8993/$ – see front matter © 2006 Elsevier B.V. All rights reserved.
doi:10.1016/j.brainres.2006.08.097

Abbreviations:
CNS, central nervous system
EAE, encephalomyelitis allergic experimental
ELISA, enzyme-linked immunosorbent assay
NO, nitric oxide
NOS, nitric oxide synthase
OD, optical density
RT-PCR, reverse transcription polymerase chain reaction
taiep, tremor, ataxia, immobility episodes, epilepsy, paralysis
TNF, tumor necrosis factor

1. Introduction

The mutant taiep rat develops a progressive neurological syndrome characterized by tremor, ataxia, immobility episodes, audiogenic seizures, and hindlimb paralysis (Holmgren et al., 1989). Hypomyelination at birth and progressive demyelination that leads to a highly hypomyelinated central nervous system (CNS) in adulthood is a feature of taiep pathology (Duncan et al., 1992; Lunn et al., 1997). The deficit in myelin has been directly associated with a cytoskeleton alteration of oligodendrocytes (Couve et al., 1997; Song et al., 1999) and with changes in expression and intracellular location of myelin gene products (Li et al., 2003; O'Connor et al., 2000).

Progressive reactive astrocytosis affecting those brain regions where hypomyelination is more severe has been shown in the taiep rat (Krsulovic et al., 1999; Leon Chavez et al., 2001). A proliferative response of activated microglia cells has also been correlated with early hypomyelination and oligodendrocyte pathology in the CNS white matter (Goetz et al., 2000). In primary cell cultures from the cerebellum, glial cells of taiep rats are able to respond more efficiently to pro-inflammatory stimuli releasing TNF-α and NO as a sign of activation of glial cells possibly caused by the myelin defect (Leon-Chavez et al., 2003). All this evidence supports the hypothesis that enhanced production of pro-inflammatory cytokines and reactive nitrogen intermediates by activated glial cells occurs in the most hypomyelinated regions of the brain of taiep rats. To date, there are no studies about reactive nitrogen intermediates in the brain of taiep rats in vivo. Because of the progression of taiep pathology (Leon Chavez et al., 2001; Lunn et al., 1997), we tested that hypothesis in the cerebellum, one of the regions primarily affected, of 6-month-old taiep rats (Duncan et al., 1992). This work analyzed the production of NO as assessed by nitrite accumulation and the expression of the three NOS isoforms by using a reverse-transcription polymerase chain reaction (RT-PCR) and an enzyme-linked immunosorbent assay (ELISA). Double immunofluorescence techniques were used to explore the cellular location of the immunoreactivity against nNOS, iNOS, and eNOS. Our results suggest that enhanced levels of NO and the three NOS isoforms may play an important role in the demyelination process of taiep rats.

2. Results

The production of NO was estimated by determining the nitrite content in supernatants of cerebellum homogenates from 6-month-old taiep and control rats. Production of NO in taiep rats was 40±12% greater than that in control rats (Fig. 1). The nitrite values were 2.55±0.07 (controls) and 3.6±0.3 (taiep rats) as expressed as μM/mg of total protein, $P<0.05$, $n=5$.

The enhanced production of NO was accompanied with an increase in protein levels of the three NOS isoforms in the cerebellum of the taiep rat as assessed by ELISA (Fig. 2). The increases were statistically significant when compared with control values and represented 18±3% for nNOS (Fig. 2A), 34±4% for iNOS (Fig. 2B), and 18±2% for eNOS (Fig. 2C). The ODs at 415 nm were 0.160±0.003 (controls) and 0.189±0.005 (taiep rats) for nNOS, 0.15±0.009 (controls) and 0.200±0.006 (taiep rats) for iNOS, and 0.170±0.005 (controls) and 0.200±0.004 (taiep rats) for eNOS.

The increased levels of the three isoforms of NOS protein were associated with the upregulation of mRNA levels in the cerebellum of the taiep rat (Fig. 3). The normalized ODs of the electrophoretic bands were 0.735±0.042 (controls) and 1.00±0.012 (taiep rats) for nNOS, 0.944±0.014 (controls) and 1.169±0.038 (taiep rats) for iNOS, and 0.723±0.024 (controls) and 0.850±0.017 (taiep rats) for eNOS. There was a statistically significant increase when the normalized values of the three

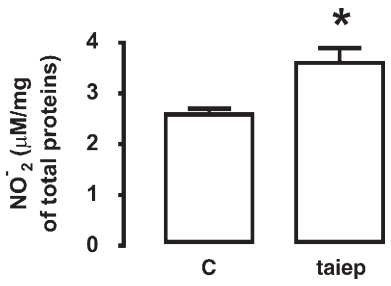

Fig. 1 – Increased nitric oxide production in the cerebellum of the taiep rat. Nitrite levels were determined by the Griess method. Each value represents the mean ± *s* of 5 independent experiments made in triplicate. C, control. *Significantly different from the control group, $P<0.05$, Student's *t*-test.

isoforms of taiep rats were compared with those of controls and was 36±2% for nNOS (Fig. 3A), 24±4% for iNOS (Fig. 3B), and 18±2% for eNOS (Fig. 3C).

To establish differences of the immunostained cells of taiep rats, we decided to analyze the immunoreactivity for nNOS in the granular layer of the cerebellum and that for iNOS in the Purkinje layer, where nNOS-IR cells (Chung et al., 2002; Rodrigo et al., 2001; Suarez et al., 2005) and iNOS-IR cells (Rodrigo et al., 2001; Shin et al., 2004; Suarez et al., 2005) have been well-known for some time in control rats. In cerebellum sections of 6-month-old control rats, nNOS-IR was located mainly in neurons of the granular layer, as expected (Rodrigo et al., 2001). Less frequently, nNOS-IR was also observed in perivascular glial cells, but not in cytoplasmic astrocytes (Figs. 4A–C). The iNOS-IR was found in Purkinje cells (Figs. 4H and I), barely in perivascular glial cells, but not in Bergman cells (data not shown). The eNOS-IR was located in the Bergman glia and astrocytes (data not shown). In taiep rats, an increased number of perivascular and cytoplasmic astrocytes of the granular layer showed nNOS-IR (Figs. 4D–F). The nNOS-IR was also observed in neurons (Figs. 4E–F). The iNOS-IR was found more frequently in perivascular glial cells (data not shown) and in cytoplasmic astrocytes of the Purkinje layer, but not in Bergman glia (Figs. 4J–L). Similarly to control rats, iNOS-IR was observed in Purkinje cells of taiep rats (Figs. 4K and L). The eNOS-IR was found within the Bergman glia and astrocytes, as seen in controls (data not shown).

The presence of professional immune cells in the cerebellum of taiep rats as other possible sources of NOS isoforms was explored in the cerebellar white matter, a region affected by the demyelination in the taiep rat (Duncan et al., 1992).

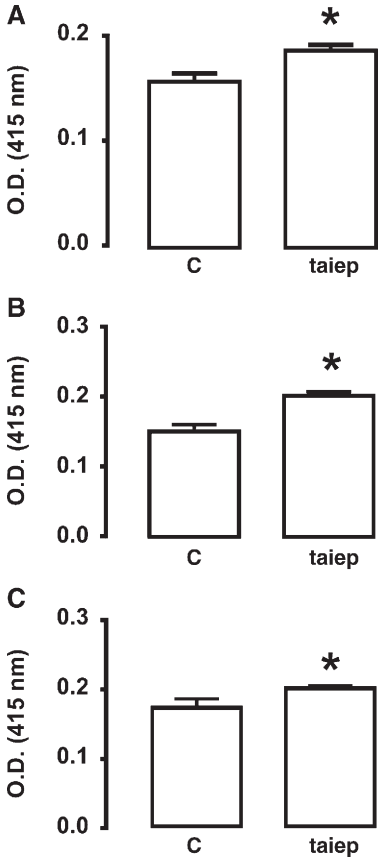

Fig. 2 – Increased levels of NOS isoform proteins in the cerebellum of the taiep rat. ELISA was used to determine the protein levels of nNOS (A), iNOS (B), and eNOS (C) in separate assays. The primary antibodies to different NOS isoforms were raised in mice. The secondary antibody was a goat anti-IgG mouse PRH conjugated. Each value represents the mean ± *s* of 5 independent experiments made in triplicate. C, control. *Significantly different from the control group, *P*<0.05, Student's *t*-test.

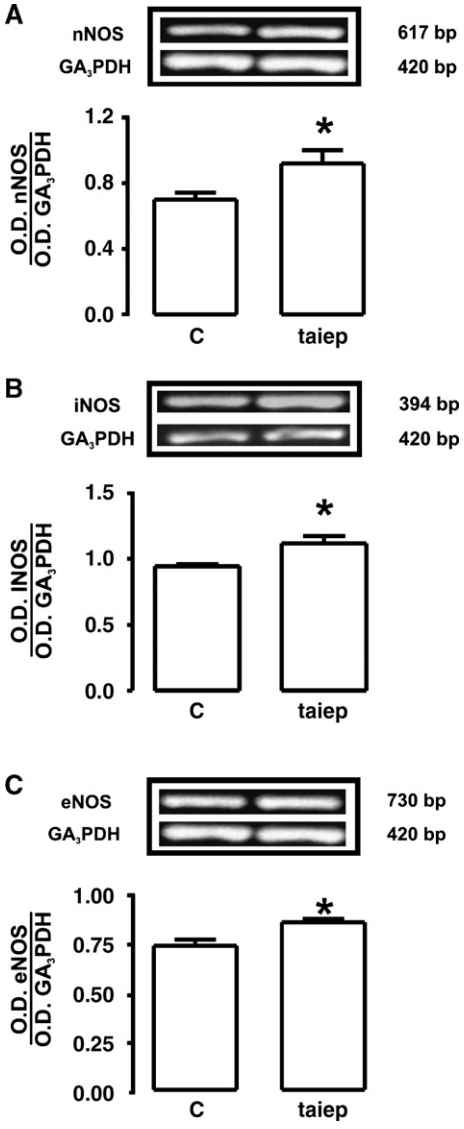

Fig. 3 – Upregulation of mRNA for NOS isoforms in the cerebellum of the taiep rat. RT-PCR was used to determine mRNA levels for nNOS (A), iNOS (B), and eNOS (C). Each panel shows both a representative photograph of ethidium–bromide-stained RT-PCR products fractionated on 2% agarose gel and the graph of densitometry analysis. Each value represents the mean ± *s* of 5 independent experiments made in triplicate. C, control. *Significantly different from the control group, *P*<0.05, Student's *t*-test.

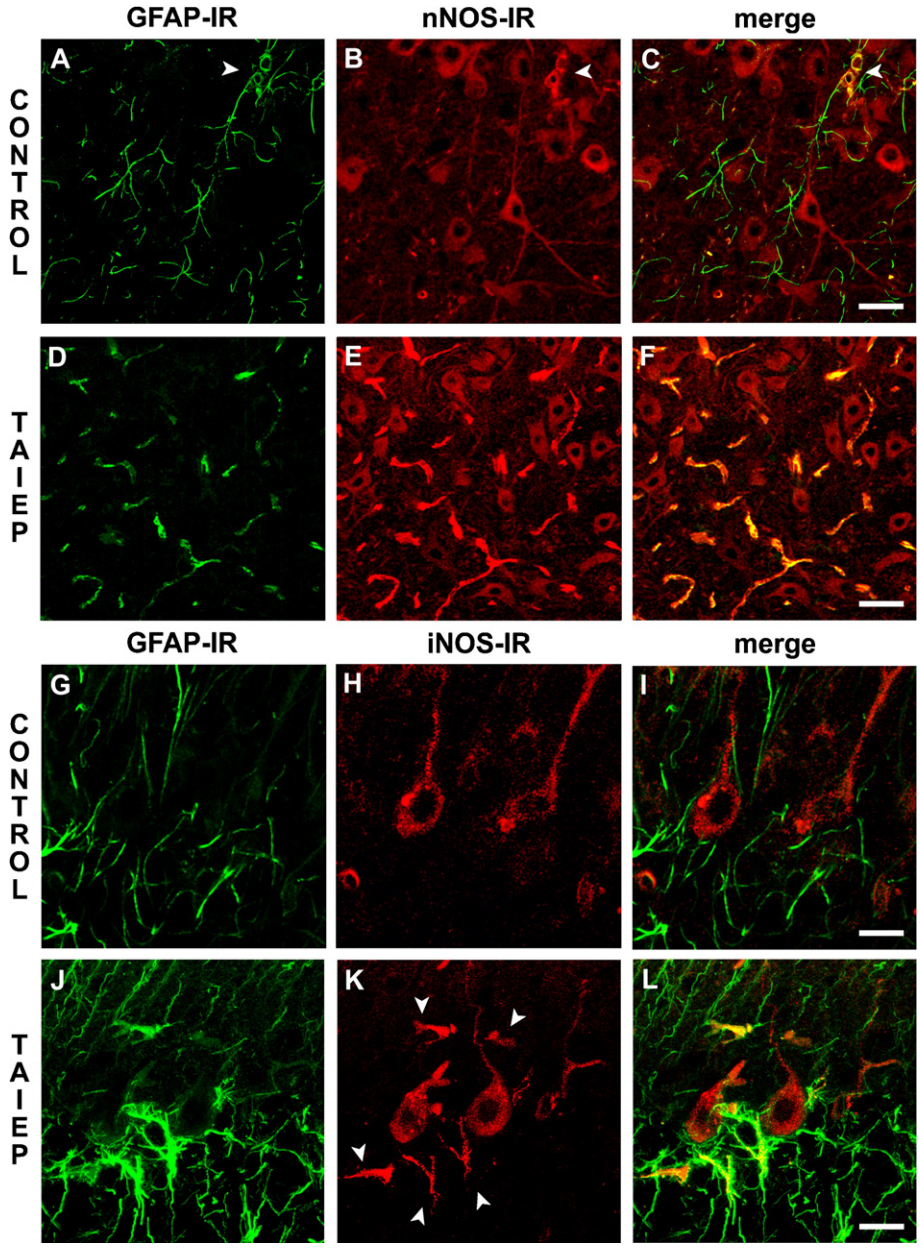

Fig. 4 – Cell location of the immunoreactivity of nNOS and iNOS in the granular and Purkinje layers of the cerebellum. Immunostaining for nNOS was assessed in the granular layer of both control (A–C) and taiep rats (D–F), whereas that for iNOS was assessed in the Purkinje layer of both control (G–I) and taiep rats (J–L). Overlayed images of double immunostaining of glial cells and nNOS protein show colocation of those immunorelativities (the arrowhead in panels A and B) only in the perivascular astrocytes of control rats (C) and in most of the cytoplasmic astrocytes of taiep rats (yellow cells in panel F). Overlayed images of double immunostaining of glial cells and iNOS protein show colocation of those immunoreactivities in an increased number of cytoplasmic astrocytes (arrowheads in panel K and yellow cells in panel L), but not in Bergman cells of taiep rats. In contrast, those cells were not double-immunoreactive in control rats (I). The micrographs are representative of three independent experiments. GFAP-IR = GFAP immunoreactivity; nNOS-IR = nNOS immunoreactivity; iNOS-IR = iNOS immunoreactivity. The scale bars correspond to 20 μm.

Indirect immunofluorescence techniques against CD11b (microglia–macrophage), CD4 (helper lymphocyte), and CD8 (cytotoxic lymphocyte) were assessed in slices of cerebellum of both control and taiep rats. In contrast to controls (Figs. 5A–C), an increased number of OX42-IR cells was found in the white matter of the taiep rat cerebellum (Figs. 5D–F). Because the OX42 antibody recognizes CD11b, also known as C3bi receptor or integrin alpha M chain of MAC-1, located in the macrophage in the rat (Matsumoto et al., 1992), its positive immunoreactivity shows the presence of microglia–macrophage in the cerebellar white matter of taiep rats. In the cerebellar white matter of taiep rats, cells showing IR against

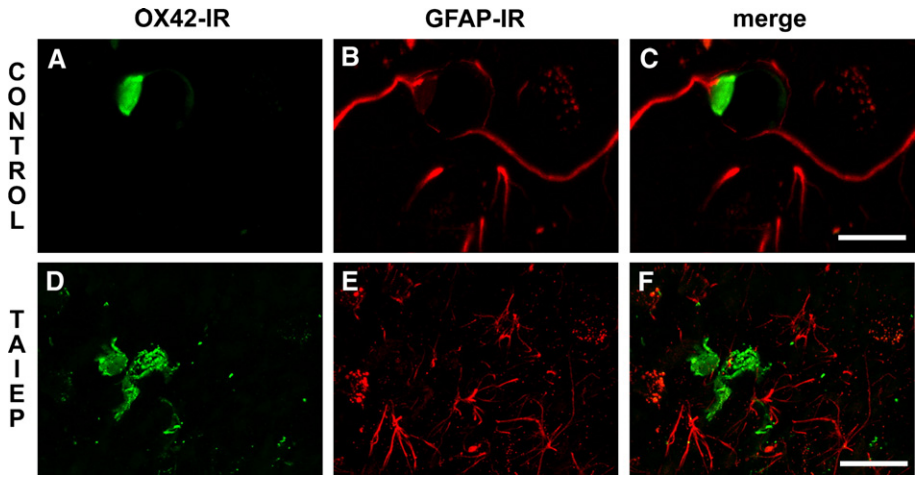

Fig. 5 – Presence of microglia–macrophages in the cerebellar parenchyma of adult taiep rats. The representative micrographs of three independent experiments show double immunostaining for microglia–macrophages (OX42-IR) and astrocytes (GFAP-IR) in the white matter of the cerebellum. The overlayed images show an increased number of OX42-IR cells in the white matter of taiep rats (F) when compared with the matched region of control cerebellum (C). OX42-IR = OX42 immunoreactivity. GFAP-IR = GFAP immunoreactivity. The scale bars correspond to 25 μm.

CD4 (Fig. 6A) and CD8 (Fig. 6C), but not in that of controls (Figs. 5B and D), were found in 6-month-old rats, suggesting the infiltration of peripheral immune cells.

3. Discussion

Our results strongly suggest that the enhanced expression of the three NOS isoforms as shown by RT-PCR and ELISA techniques contributes to the increase in NO production in the cerebellum of 6-month-old taiep rats. These findings in vivo agree with results in vitro showing that the activated glial cells from the cerebellum of taiep rats are one of the sources of the enhanced production of NO through iNOS expression. The same cellular type can be involved in the enhanced production of NO in vivo because of the presence of activated microglia (Goetz et al., 2000) and astrocytes (Krsulovic et al., 1999; Leon Chavez et al., 2001) in the cerebellum of aged taiep rats. Experimental evidence supports that activated microglia and astrocytes are the mediators of immune response in the CNS

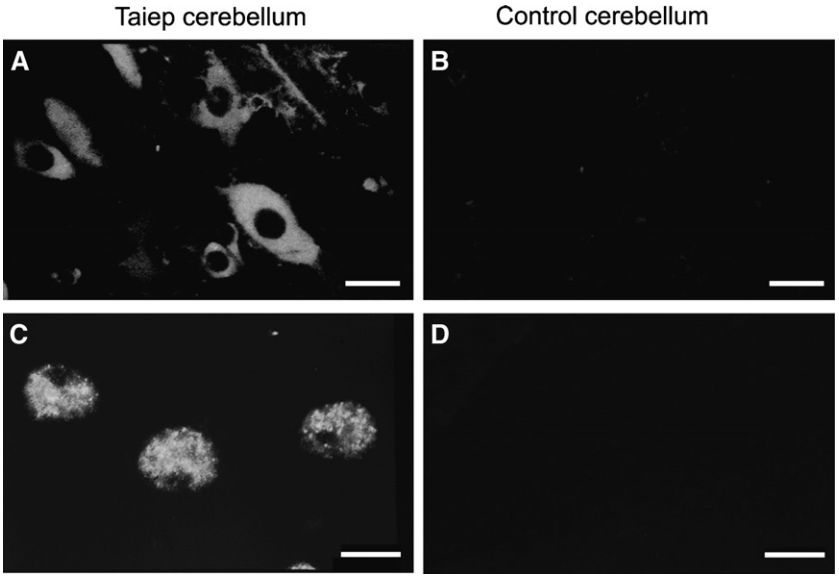

Fig. 6 – Presence of professional immune cells in the cerebellar parenchyma of adult taiep rats. Separate sections of the cerebellum of taiep and control rats were immunostained against cluster differentiation markers for either helper lymphocytes (CD4) or cytotoxic lymphocytes (CD8). The representative micrographs show the immunoreactivity to CD4 (panels A and B) and CD8 (panels C and D) in the cerebellar white matter ($n=3$). The primary antibodies were a mouse monoclonal anti-CD4 or a mouse anti-CD8, and the secondary antibody was a FITC–anti-mouse IgG. The fluorescence within the cells was detected at Ex-Em wavelengths of 488–522 nm by confocal microscopy. The calibration bar = 10 μm.

(Aschner, 1998; Chao et al., 1992). This response should be considered as an additional factor participating in the progression of taiep demyelination, as suggested by studies in vitro (Leon-Chavez et al., 2003) and in vivo (Bo et al., 1994; Hill et al., 2004; Zhang et al., 2001). The professional immune response can be also considered as a demyelinating factor in aged taiep rats because of the presence of CD4- and CD8-IR cells and microglia–macrophage in the cerebellar parenchyma as shown herein. However, the CD4-IR cells in the taiep rat do not have the typical morphology of lymphocytes (Fig. 6A). Some authors have shown the presence of the CD4 antigen in microglia–macrophages (Dick et al., 1997; Jordan et al., 1991) and neurons of the brain of the adult mouse (Omri et al., 1994). Because CD4 immunoreactivity was assessed in the white matter of the taiep rat cerebellum, we can suggest that those CD4-IR cells might correspond to either lymphocytes or activated microglia.

Our immunolabeling results showed that the three isoforms of NOS are expressed by the cerebellar cells, including neurons and astrocytes of both adult control and taiep rats. In agreement with previous findings (Saxon and Beitz, 1994; Suarez et al., 2005), the immunostaining for nNOS clearly revealed neuron cells in the granular layer of the cerebellum of control rats (Figs. 4A–C), but not in the Purkinje layer (data not shown). In contrast, the immunostaining for iNOS was found in the Purkinje cells (Figs. 4G–I), but not in the granular cells of control rats. These results also agree with previous findings (Rodrigo et al., 2001; Shin et al., 2004; Suarez et al., 2005). The intracytoplasmic nNOS immunoreactivity of granular cells (Fig. 4B) and iNOS immunoreactivity of Purkinje cell bodies and the proximal dendritic segment (Fig. 4H) have been known for some time (Chung et al., 2002; Kaur et al., 2005; Rodrigo et al., 2001; Shin et al., 2004). The intracytoplasmic location of nNOS and iNOS (Forstermann et al., 1991; Hecker et al., 1994) can account for the preferential cellular immunostainings. Though iNOS is mainly soluble, nNOS is associated with the endoplasmic reticulum (Hecker et al., 1994).

The presence of iNOS in neuronal cell types in the cerebellum and hippocampus of adult and aged rats was previously reported by others (Siles et al., 2002; Vernet et al., 1998). In our work, the presence of iNOS-IR was observed within Purkinje cells of both 6-month-old control and taiep rats. This result agrees with the increase of iNOS in adult and aged rats (Siles et al., 2002; Vernet et al., 1998) and supports the hypothesis that this isoform may lead to neurotoxicity and also act as possible cause of age-associated neuronal loss in the brain (Vernet et al., 1998). A clear difference from control cerebellum sections is that perivascular and cytoplasmic astrocytes showing nNOS- and iNOS-IR are more frequently found in cerebellum sections of taiep rats. These results strongly suggest that these cells can account for the enhanced expression of the three NOS isoforms shown by ELISA and RT-PCR techniques, and consequently for the enhanced NO levels.

In rats with experimental autoimmune encephalomyelitis (EAE), a model of human demyelinating diseases (Lublin, 1985), infiltration of T cells and macrophages and activation of microglia and astrocytes have been demonstrated at the peak stage of EAE (Ohmori et al., 1992; Shin et al., 1995). These cells, which are potent producers of NO in the brain, are suggested to be the possible sources for both nNOS and iNOS in the course of EAE (Kim et al., 2000; Teixeira et al., 2002). In addition to NO, those cells releasing pro-inflammatory cytokines (Kim et al., 2004; Lee et al., 2005; Sun et al., 2005), known to be directly associated with demyelination (Zhang et al., 2001), cause the myelin deficit. Our immunostaining for OX42 shows an increased number of microglia–macrophages in the cerebellar white matter of the taiep rat (Figs. 5D–F), thus indicating the infiltration of these cells in the region affected by demyelination (Duncan et al., 1992). Similar to EAE, the enhanced NO production and NOS expression by infiltrated T cells, microglia–macrophages, and activated astrocytes may also contribute to the progression of demyelination in the taiep rat, an innate model of chronic demyelination.

Because NO can produce either cytoprotection or cytotoxicity (Bo et al., 1994; Kim et al., 1999; Sun et al., 1998; Svenningsson et al., 1999), which of these plays in the demyelination of taiep rats is not yet known. Studies in vitro have shown that increased NO levels, by acting as a mediator of oxidative stress, are able to produce cytotoxicity in neurons, astrocytes, and oligodendrocytes (Boje and Arora, 1992; Dawson et al., 1994; Merrill et al., 1993). These findings together with evidence in vivo (Blais and Rivest, 2004; Hill et al., 2004; Smith and Lassmann, 2002) support the hypothesis that NO from an iNOS source leads to intense neurodegeneration and demyelination. On the contrary, the cytoprotection by NO as source of constitutive NOS is supported by several studies on experimental allergic encephalomyelitis (Kim et al., 2000). The stasis of T cell proliferation may be one of the mechanisms involved in the cytoprotection by NO (Kim et al., 2000). The iNOS isoform has also been involved in NO cytoprotection as shown by the exacerbation of demyelination in nonautoimmune models caused by either the inactivation of iNOS or the lack of the iNOS gene (Arnett et al., 2002; Fenyk-Melody et al., 1998; O'Brien et al., 2001; Sahrbacher et al., 1998).

In summary, the main conclusion that emerges from our study is that the three NOS isoforms participate in the enhanced production of NO in the cerebellum, a severe demyelinated region, of the taiep rat. Activated microglia and astrocytes, and T cells may be the source to the enhanced NOS expression and NO production, thus contributing to the demyelinating processes of aged taiep rats. The taiep rat, an innate chronic demyelination model, provides a tool to explore the mechanisms of immune response in the CNS.

4. Experimental procedures

4.1. *Experimental animals*

Six-month-old taiep rats were obtained from the vivarium of the Institute of Physiology, BUAP. Animals were maintained in rooms with controlled conditions of temperature (22±1 °C) and light–dark cycle (12:12-h light–dark; light onset at 0700). Food and water were provided ad libitum. All procedures were in accordance with the Mexican current legislation, the NOM-062-ZOO-1999 (SAGARPA), based on the Guide for the Care and Use of Laboratory Animals, NRC. Aged-matched Sprague-Dawley rats were from The CINVESTAV Institutional Animal Care and Use Committee (IACUC), which approved our animal use procedures with the protocol number 0109-02. All efforts were made to minimize animal suffering.

4.2. *Nitric oxide determination*

Cerebella of control or taiep rats ($n=5$ in each group) were mechanically homogenized in phosphate-buffered saline solution, pH 7.4 (PBS), and centrifuged at 12,500 rpm for 30 min at 4 °C by using a 17TR microcentrifuge (Hanil Science Industrial Co, Ltd.; Inchun, Korea). The NO production was assessed by the accumulation of nitrites (NO_2^-) in supernatants of homogenates as described elsewhere (Gonzalez-Barrios et al., 2002; Leon-Chavez et al., 2003). Briefly, nitrite concentration in 100 μl of supernatant was measured by using a colorimetric reaction generated by the addition of 100 μl of Griess reagent, which was composed of equal volumes of 0.1% N-(1-naphthyl) ethylenediamine dihydrochloride and 1.32% sulfanilamide in 60% acetic acid. The absorbance of the samples was determined at 500 nm with a SmartSpec 3000 spectrophotometer (Bio-Rad, Hercules, CA, USA) and interpolated by using a standard curve of $NaNO_2$ (1 to 10 μM) to calculate the nitrite content.

4.3. *Enzyme-linked immunosorbent assay*

ELISA was used to determine the three isoforms of NOS in homogenates of cerebella of control or taiep rats ($n=5$ in each group) as we described previously (Leon Chavez et al., 2001; Leon-Chavez et al., 2003).The protein content was determined using the method described elsewhere (Sedmak and Grossberg, 1977). Aliquots containing 5 μg of total protein were placed into wells of ELISA plates for the separate determination of nNOS, iNOS, and eNOS. Volumes of 100 μl of 0.1 M carbonate buffer were added into each well and the plate was incubated for 18 h at 4 °C. To block nonspecific binding sites, 200 μl of 0.5% bovine serum albumin, IgG free, was added to each well at room temperature (RT). After 30-min incubation, the wells were washed three times with PBS–Tween 20 (0.1%). Mouse monoclonal antibodies to nNOS, iNOS, or eNOS (1:200 dilution; Sigma-Aldrich Co.; St. Louis, MO, USA) were added into each well and incubated for 2 h at RT. After three washings with PBS, a horseradish-peroxidase-conjugated goat anti-mouse IgG (1:1000 dilution; Dako A/S Denmark (Dako North America, Inc. Carpinteria, CA) was added and incubated for 2 h at RT. The antibody–antigen complex was revealed by adding 100 μl of ABTS containing 0.3% H_2O_2 into each well. After 15 min, optical density (OD) was determined at 415 nm using a Benchmark multiplate reader (Bio-Rad, Hercules, CA, USA) as described (Leon-Chavez et al., 2003).

4.4. *Reverse transcriptase-polymerase chain reaction*

The RT-PCR technique was used to determine mRNA levels of the three isoforms of NOS in homogenates of cerebella of control or taiep rats ($n=5$ in each group) as described elsewhere (Gonzalez-Barrios et al., 2002; Leon-Chavez et al., 2003). Total RNA was isolated from 100 mg of tissue in 1 ml of TRizol reagent (Invitrogene, Carlsbad, CA, USA), quantified by spectrophotometry at 260 nm, and analyzed by 2% agarose gel electrophoresis. The RNA preparations were treated with RNase-free DNase before their use in the reverse transcription to amplify NOS isoforms and glyceraldehyde-3-phosphate dehydrogenase (GA3PDH) as the house-keeping gene, using specific primers.

To amplify a 617-bp fragment of nNOS, the sense primer was 5′-CCG GAA TTC GAA TAC CAG CCT GAT CCA TGG AA-3′ and the antisense primer was 5′-CCG AAT TCC TCC AGG AGG GTG TCC ACC GCA TG-3′ (GenBank accession no. AJ01116). These primers flank the bases 2452–2483 sense and 3068–3037 antisense (Seidel et al., 1997).

To amplify a 394-bp fragment of iNOS, the sense primer was 5′-CCA CAA TAG TAC AAT ACT ACT TGG-3′ and the antisense primer was 5′-ACG AGG TGT TCA GCG TGC TCC ACG-3′ (GenBank accession no. U03699). These primers flank the bases 3191–3214 sense and 3584–3561 antisense of the mRNA sequence for iNOS (Galea et al., 1994).

To amplify a 742-bp fragment of eNOS, the sense primer was 5′-GAG AAT TCC ACC TCA CTG TAG CTG TGC TGG CA-3′ and the antisense primer was 5′-TCG AAT TCC CAG GGC ACT GCG CCC CGC AAC TG-3′ (GenBank accession no. AJ01116). These primers flank the bases 1–32 sense and 730–698 antisense (Seidel et al., 1997).

To amplify a 420-bp fragment of GA_3PDH, the sense primer was 5′-ACC ACA GTC CAT GCC ATC AC-3′ and the antisense primer was 5′-TCC ACC ACC CTG TTG CTG TA-3′ (GenBank accession no. X59949).

The total RNA (5 μg) was transcribed with SuperScript II reverse transcriptase (200 U) using 0.1 μg of random hexamer (Invitrogene; Carlsbad, CA; USA). One μl of the reverse transcribed product was amplified in a temperature gene cycler (Gene Amp PCR System 9700; Applied Biosystems, Foster city, CA, USA) using 0.2 μM of each sense and antisense primer and 2.5 U of platinum Taq DNA polymerase in a final volume of 50 μl. After an initial denaturation at 94 °C for 2 min, amplification was made for 35 cycles as follows: 94 °C for 1 min (denaturation), 64 °C for 1 min (annealing), and 72 °C for 1 min (extension). PCR products were analyzed by restriction assays and fractionated on 2% agarose gel. Upon completion of electrophoresis, ethidium bromide-stained-PCR products were photographed with a Kodak DC290 camera (Eastman Kodak Co, Rochester, NY, USA). Densitometric analysis was accomplished with the software Quantity one 4.1.1 (Bio-Rad, Hercules, CA, USA) and the densitometric values (arbitrary units) of NOS bands were normalized with respect to the densitometric values of GA3PDH bands.

4.5. *Immunolabeling of NOS*

NOS immunoreactivity was also analyzed by indirect immunofluorescence in brain sagittal slices of 6-month-old control and taiep rats ($n=3$ in each group). Rats were deeply anesthetized with chloral hydrate and perfused through the ascending aorta with 100 ml of PBS, then by 150 ml of 4% paraformaldehyde in PBS. Their brains were removed and maintained in the fixative for 48 h at 4 °C. After overnight maintenance in PBS containing 10% sucrose at 4 °C, each brain was frozen and sectioned into 35-μm slices on the sagittal plane using a Leitz cryostat (LEICA 2000R). Slices were individually collected in a 24-well plate containing PBS and used for fluorescent immunolabeling of astroglial cells, microglial cells, and NOS isoforms. Slices were incubated

with 0.5% IgG-free bovine serum albumin in PBS–Tween 20 (0.1%) for 20 min at room temperature.

The primary antibodies were (1) the rabbit polyclonal anti-cow GFAP (1:400 dilution; catalog #Z0334; Dako; Carpinteria, CA, USA) previously used to identify astrocytes (Alvarez-Maya et al., 2001; Leon Chavez et al., 2001; Navarro-Quiroga et al., 2002), (2) the mouse monoclonal anti-nNOS (1:100 dilution; Cat. #sc-5302; Santa Cruz Biotechnology Inc.; Santa Cruz, CA, USA), whose specificity was reported by others (Molero et al., 2002), (3) the mouse monoclonal anti-iNOS (1:200 dilution; catalog #AB5384; Chemicon; Temecula, CA, USA) tested by others (Walsh et al., 2004), (4) the rabbit polyclonal anti-eNOS (1:200 dilution; catalog #N2643; Sigma-Aldrich Co.; St Louis, MO, USA), whose specificity was reported previously (Dinerman et al., 1994), (5) the mouse monoclonal OX42 antibody (1:100 dilution; Cat. #MCA275R; Serotec; Oxford, UK) that is a specific marker of microglia–macrophages (Matsumoto et al., 1992), (6) the mouse monoclonal anti-CD4 (1:200 dilution; catalog #CL038A; Cedar Lane Lab.; Hornby, Ontario, Canada), and (7) the mouse anti-CD8 of rat (1:200 dilution; catalog #CLSG36556X; Cedar Lane Lab.; Hornby, Ontario, Canada). The antibodies to CD4 and CD8 were tested by flow cytometry before their used for immunostaining.

The secondary antibodies were (1) fluorescein (FITC)– or rhodamine (Rho)–goat anti-rabbit IgG, (2) FITC–goat–anti-mouse IgG, and (3) rhodamine (Rho)-conjugated goat anti-mouse IgG (1:60 dilution; Pierce Technology Co.; Holmdel, NJ, USA).

Double immunofluorescence studies were done combining suitable primary and secondary antibodies to avoid cross-reactivity. Because of the lack of primary antibodies to eNOS different from the rabbit source, double immunostaining against eNOS and glial cells was not done. Slices were mounted on glass slides using vectashield (Vector Laboratories; Burlington, Ontario, Canada) and analyzed on a confocal imaging system equipped with a krypton–argon laser beam (Bio-Rad MRC-600, Watford, UK) as we have described elsewhere (Navarro-Quiroga et al., 2002). The fluorescence was detected at Ex-Em wavelengths of 488–522 nm (green channel) and 568–585 nm (red channel). Ten to twenty consecutive optical sections at 1-μm intervals were obtained in the z-series. The resulting images were projected in a bidimensional plane and were overlapped on the screen monitor using green for FITC and red for Rho. Brain sections processed under similar conditions in the absence of the primary antibody were used as negative controls.

4.6. *Statistical analysis*

All values are means ± s obtained from at least 5 independent experiments. After testing for normality with the Snedecor's F-analysis, the significance of differences was analyzed by the unpaired Student's t-test. The significance was considered at $P < 0.05$.

Acknowledgments

This work was supported by the grant J-34143 (B.A.L.-C.) and 43674-A (J.R.E.) from CONACYT and VIEP-BUAP I/G/SAL/05 A (J.R.E.). Patricia Aguilar-Alonso and Juan A. Gonzalez-Barrios were recipient of scholarships from CONACYT. We thank M. C. Nidia Pazos for her technical assistance and The Institute of Physiology of BUAP for the production and maintenance of taiep rats. Thanks to Dr. Ellis Glazier for editing of the English-language text.

REFERENCES

Alvarez-Maya, I., Navarro-Quiroga, I., Meraz-Rios, M.A., Aceves, J., Martinez-Fong, D., 2001. In vivo gene transfer to dopamine neurons of rat substantia nigra via the high-affinity neurotensin receptor. Mol. Med. 7, 186–192.

Arnett, H.A., Hellendall, R.P., Matsushima, G.K., Suzuki, K., Laubach, V.E., Sherman, P., Ting, J.P., 2002. The protective role of nitric oxide in a neurotoxicant-induced demyelinating model. J. Immunol. 168, 427–433.

Aschner, M., 1998. Immune and inflammatory responses in the CNS: modulation by astrocytes. Toxicol. Lett. 102–103, 283–287.

Blais, V., Rivest, S., 2004. Effects of TNF-alpha and IFN-gamma on nitric oxide-induced neurotoxicity in the mouse brain. J. Immunol. 172, 7043–7052.

Bo, L., Dawson, T.M., Wesselingh, S., Mork, S., Choi, S., Kong, P.A., Hanley, D., Trapp, B.D., 1994. Induction of nitric oxide synthase in demyelinating regions of multiple sclerosis brains. Ann. Neurol. 36, 778–786.

Boje, K.M., Arora, P.K., 1992. Microglial-produced nitric oxide and reactive nitrogen oxides mediate neuronal cell death. Brain Res. 587, 250–256.

Chao, C.C., Hu, S., Molitor, T.W., Shaskan, E.G., Peterson, P.K., 1992. Activated microglia mediate neuronal cell injury via a nitric oxide mechanism. J. Immunol. 149, 2736–2741.

Chung, Y.H., Shin, C.M., Joo, K.M., Kim, M.J., Cha, C.I., 2002. Immunohistochemical study on the distribution of nitrotyrosine and neuronal nitric oxide synthase in aged rat cerebellum. Brain Res. 951, 316–321.

Couve, E., Cabello, J.F., Krsulovic, J., Roncagliolo, M., 1997. Binding of microtubules to transitional elements in oligodendrocytes of the myelin mutant taiep rat. J. Neurosci. Res. 47, 573–581.

Dawson, V.L., Brahmbhatt, H.P., Mong, J.A., Dawson, T.M., 1994. Expression of inducible nitric oxide synthase causes delayed neurotoxicity in primary mixed neuronal–glial cortical cultures. Neuropharmacology 33, 1425–1430.

Dick, A.D., Pell, M., Brew, B.J., Foulcher, E., Sedgwick, J.D., 1997. Direct ex vivo flow cytometric analysis of human microglial cell CD4 expression: examination of central nervous system biopsy specimens from HIV-seropositive patients and patients with other neurological disease. AIDS 11, 1699–1708.

Dinerman, J.L., Dawson, T.M., Schell, M.J., Snowman, A., Snyder, S.H., 1994. Endothelial nitric oxide synthase localized to hippocampal pyramidal cells: implications for synaptic plasticity. Proc. Natl. Acad. Sci. U. S. A. 91, 4214–4218.

Duncan, I.D., Lunn, K.F., Holmgren, B., Urba-Holmgren, R., Brignolo-Holmes, L., 1992. The taiep rat: a myelin mutant with an associated oligodendrocyte microtubular defect. J. Neurocytol. 21, 870–884.

Fenyk-Melody, J.E., Garrison, A.E., Brunnert, S.R., Weidner, J.R., Shen, F., Shelton, B.A., Mudgett, J.S., 1998. Experimental autoimmune encephalomyelitis is exacerbated in mice lacking the NOS2 gene. J. Immunol. 160, 2940–2946.

Forstermann, U., Pollock, J.S., Schmidt, H.H., Heller, M., Murad, F., 1991. Calmodulin-dependent endothelium-derived relaxing factor/nitric oxide synthase activity is present in the particulate and cytosolic fractions of bovine aortic endothelial cells. Proc. Natl. Acad. Sci. U. S. A. 88, 1788–1792.

Galea, E., Reis, D.J., Feinstein, D.L., 1994. Cloning and expression of inducible nitric oxide synthase from rat astrocytes. J. Neurosci. Res. 37, 406–414.

Goetz, B.D., Zhang, S.C., Song, J., Duncan, I.D., 2000. Microglial response to progressive demyelination in the taiep mutant rat. Program No. 515. 7. 2000 Abstract Viewer/Itinerary Planner. Washington, DC: Society for Neuroscience. Online. 30th Annual meeting of Society for Neurosciences. (2000) New Orleans, LA. USA.

Gonzalez-Barrios, J.A., Escalante, B., Valdes, J., Leon-Chavez, B.A., Martinez-Fong, D., 2002. Nitric oxide and nitric oxide synthases in the fetal cerebral cortex of rats following transient uteroplacental ischemia. Brain Res. 945, 114–122.

Hecker, M., Mulsch, A., Busse, R., 1994. Subcellular localization and characterization of neuronal nitric oxide synthase. J. Neurochem. 62, 1524–1529.

Hill, K.E., Zollinger, L.V., Watt, H.E., Carlson, N.G., Rose, J.W., 2004. Inducible nitric oxide synthase in chronic active multiple sclerosis plaques: distribution, cellular expression and association with myelin damage. J. Neuroimmunol. 151, 171–179.

Holmgren, B., Urba-Holmgren, R., Riboni, L., Vega-SaenzdeMiera, E.C., 1989. Sprague Dawley rat mutant with tremor, ataxia, tonic immobility episodes, epilepsy and paralysis. Lab. Anim. Sci. 39, 226–228.

Jordan, C.A., Watkins, B.A., Kufta, C., Dubois-Dalcq, M., 1991. Infection of brain microglial cells by human immunodeficiency virus type 1 is CD4 dependent. J. Virol. 65, 736–742.

Kaur, C., Sivakumar, V., Singh, G., Singh, J., Ling, E.A., 2005. Response of Purkinje neurons to hypobaric hypoxic exposure as shown by alteration in expression of glutamate receptors, nitric oxide synthases and calcium binding proteins. Neuroscience 135, 1217–1229.

Kim, Y.M., Chung, H.T., Kim, S.S., Han, J.A., Yoo, Y.M., Kim, K.M., Lee, G.H., Yun, H.Y., Green, A., Li, J., Simmons, R.L., Billiar, T.R., 1999. Nitric oxide protects PC12 cells from serum deprivation-induced apoptosis by cGMP-dependent inhibition of caspase signaling. J. Neurosci. 19, 6740–6747.

Kim, S., Moon, C., Wie, M.B., Kim, H., Tanuma, N., Matsumoto, Y., Shin, T., 2000. Enhanced expression of constitutive and inducible forms of nitric oxide synthase in autoimmune encephalomyelitis. J. Vet. Sci. 1, 11–17.

Kim, W.K., Jang, P.G., Woo, M.S., Han, I.O., Piao, H.Z., Lee, K., Lee, H., Joh, T.H., Kim, H.S., 2004. A new anti-inflammatory agent KL-1037 represses proinflammatory cytokine and inducible nitric oxide synthase (iNOS) gene expression in activated microglia. Neuropharmacology 47, 243–252.

Krsulovic, J., Couve, E., Roncagliolo, M., 1999. Dysmyelination, demyelination and reactive astrogliosis in the optic nerve of the taiep rat. Biol. Res. 32, 253–262.

Lee, C.J., Lee, S.S., Chen, S.C., Ho, F.M., Lin, W.W., 2005. Oregonin inhibits lipopolysaccharide-induced iNOS gene transcription and upregulates HO-1 expression in macrophages and microglia. Br. J. Pharmacol. 146, 378–388.

Leon Chavez, B.A., Guevara, J., Galindo, S., Luna, J., Ugarte, A., Villegas, O., Mena, R., Eguibar, J.R., Martinez-Fong, D., 2001. Regional and temporal progression of reactive astrocytosis in the brain of the myelin mutant taiep rat. Brain Res. 900, 152–155.

Leon-Chavez, B.A., Antonio Gonzalez-Barrios, J., Ugarte, A., Meraz, M.A., Martinez-Fong, D., 2003. Evidence in vitro of glial cell priming in the taiep rat. Brain Res. 965, 274–278.

Li, F.Y., Song, J., Duncan, I.D., 2003. Mapping of taiep rat phenotype to rat Chromosome 9. Mamm. Genome 14, 703–705.

Lublin, F.D., 1985. Relapsing experimental allergic encephalomyelitis. An autoimmune model of multiple sclerosis. Springer Semin. Immunopathol. 8, 197–208.

Lunn, K.F., Clayton, M.K., Duncan, I.D., 1997. The temporal progression of the myelination defect in the taiep rat. J. Neurocytol. 26, 267–281.

Matsumoto, Y., Ohmori, K., Fujiwara, M., 1992. Microglial and astroglial reactions to inflammatory lesions of experimental autoimmune encephalomyelitis in the rat central nervous system. J. Neuroimmunol. 37, 23–33.

Merrill, J.E., Ignarro, L.J., Sherman, M.P., Melinek, J., Lane, T.E., 1993. Microglial cell cytotoxicity of oligodendrocytes is mediated through nitric oxide. J. Immunol. 151, 2132–2141.

Molero, L., Garcia-Duran, M., Diaz-Recasens, J., Rico, L., Casado, S., Lopez-Farre, A., 2002. Expression of estrogen receptor subtypes and neuronal nitric oxide synthase in neutrophils from women and men: regulation by estrogen. Cardiovasc. Res. 56, 43–51.

Navarro-Quiroga, I., Gonzalez-Barrios, J.A., Barron-Moreno, F., Gonzalez-Bernal, V., Martinez-Arguelles, D.B., Martinez-Fong, D., 2002. Improved neurotensin-vector-mediated gene transfer by the coupling of hemagglutinin HA2 fusogenic peptide and Vp1 SV40 nuclear localization signal. Mol. Brain Res. 105, 86–97.

O'Brien, N.C., Charlton, B., Cowden, W.B., Willenborg, D.O., 2001. Inhibition of nitric oxide synthase initiates relapsing remitting experimental autoimmune encephalomyelitis in rats, yet nitric oxide appears to be essential for clinical expression of disease. J. Immunol. 167, 5904–5912.

O'Connor, L.T., Goetz, B.D., Couve, E., Song, J., Duncan, I.D., 2000. Intracellular distribution of myelin protein gene products is altered in oligodendrocytes of the taiep rat. Mol. Cell. Neurosci. 16, 396–407.

Ohmori, K., Hong, Y., Fujiwara, M., Matsumoto, Y., 1992. In situ demonstration of proliferating cells in the rat central nervous system during experimental autoimmune encephalomyelitis. Evidence suggesting that most infiltrating T cells do not proliferate in the target organ. Lab. Invest. 66, 54–62.

Omri, B., Crisanti, P., Alliot, F., Marty, M.C., Rutin, J., Levallois, C., Privat, A., Pessac, B., 1994. CD4 expression in neurons of the central nervous system. Int. Immunol. 6, 377–385.

Rodrigo, J., Alonso, D., Fernandez, A.P., Serrano, J., Richart, A., Lopez, J.C., Santacana, M., Martinez-Murillo, R., Bentura, M.L., Ghiglione, M., Uttenthal, L.O., 2001. Neuronal and inducible nitric oxide synthase expression and protein nitration in rat cerebellum after oxygen and glucose deprivation. Brain Res. 909, 20–45.

Sahrbacher, U.C., Lechner, F., Eugster, H.P., Frei, K., Lassmann, H., Fontana, A., 1998. Mice with an inactivation of the inducible nitric oxide synthase gene are susceptible to experimental autoimmune encephalomyelitis. Eur. J. Immunol. 28, 1332–1338.

Saxon, D.W., Beitz, A.J., 1994. Cerebellar injury induces NOS in Purkinje cells and cerebellar afferent neurons. Neuroreport 5, 809–812.

Sedmak, J.J., Grossberg, S.E., 1977. A rapid, sensitive, and versatile assay for protein using Coomassie brilliant blue G250. Anal. Biochem. 79, 544–552.

Seidel, B., Stanarius, A., Wolf, G., 1997. Differential expression of neuronal and endothelial nitric oxide synthase in blood vessels of the rat brain. Neurosci. Lett. 239, 109–112.

Shin, T., Kojima, T., Tanuma, N., Ishihara, Y., Matsumoto, Y., 1995. The subarachnoid space as a site for precursor T cell proliferation and effector T cell selection in experimental autoimmune encephalomyelitis. J. Neuroimmunol. 56, 171–178.

Shin, T., Weinstock, D., Castro, M.D., Hamir, A.N., Wampler, T., Walter, M., Kim, H.Y., Acland, H., 2004. Immunohistochemical localization of endothelial and inducible nitric oxide synthase within neurons of cattle with rabies. J. Vet. Med. Sci. 66, 539–541.

Siles, E., Martinez-Lara, E., Canuelo, A., Sanchez, M., Hernandez, R., Lopez-Ramos, J.C., Del Moral, M.L., Esteban, F.J., Blanco, S., Pedrosa, J.A., Rodrigo, J., Peinado, M.A., 2002. Age-related changes of the nitric oxide system in the rat brain. Brain Res. 956, 385–392.

Smith, K.J., Lassmann, H., 2002. The role of nitric oxide in multiple sclerosis. Lancet Neurol. 1, 232–241.

Song, J., O'Connor, L.T., Yu, W., Baas, P.W., Duncan, I.D., 1999. Microtubule alterations in cultured taiep rat oligodendrocytes lead to deficits in myelin membrane formation. J. Neurocytol. 28, 671–683.

Suarez, I., Bodega, G., Rubio, M., Felipo, V., Fernandez, B., 2005. Neuronal and inducible nitric oxide synthase expression in the rat cerebellum following portacaval anastomosis. Brain Res. 1047, 205–213.

Sun, D., Coleclough, C., Cao, L., Hu, X., Sun, S., Whitaker, J.N., 1998. Reciprocal stimulation between TNF-alpha and nitric oxide may exacerbate CNS inflammation in experimental autoimmune encephalomyelitis. J. Neuroimmunol. 89, 122–130.

Sun, K.H., Tang, S.J., Chen, C.Y., Lee, T.P., Feng, C.K., Yu, C.L., Sun, G.H., 2005. Monoclonal ribosomal P autoantibody inhibits the expression and release of IL-12, TNF-alpha and iNOS in activated RAW macrophage cell line. J. Autoimmun. 24, 135–143.

Svenningsson, A., Petersson, A.S., Andersen, O., Hansson, G.K., 1999. Nitric oxide metabolites in CSF of patients with MS are related to clinical disease course. Neurology 53, 1880–1882.

Teixeira, S.A., Castro, G.M., Papes, F., Martins, M.L., Rogerio, F., Langone, F., Santos, L.M., Arruda, P., de Nucci, G., Muscara, M.N., 2002. Expression and activity of nitric oxide synthase isoforms in rat brain during the development of experimental allergic encephalomyelitis. Brain Res. Mol. Brain Res. 99, 17–25.

Vernet, D., Bonavera, J.J., Swerdloff, R.S., Gonzalez-Cadavid, N.F., Wang, C., 1998. Spontaneous expression of inducible nitric oxide synthase in the hypothalamus and other brain regions of aging rats. Endocrinology 139, 3254–3261.

Walsh, K.A., Megyesi, J.F., Wilson, J.X., Crukley, J., Laubach, V.E., Hammond, R.R., 2004. Antioxidant protection from HIV-1 gp120-induced neuroglial toxicity. J. Neuroinflammation 1, 8.

Zhang, S.C., Goetz, B.D., Carre, J.L., Duncan, I.D., 2001. Reactive microglia in dysmyelination and demyelination. Glia 34, 101–109.